

# Analyst

Accepted Manuscript



This is an *Accepted Manuscript*, which has been through the Royal Society of Chemistry peer review process and has been accepted for publication.

*Accepted Manuscripts* are published online shortly after acceptance, before technical editing, formatting and proof reading. Using this free service, authors can make their results available to the community, in citable form, before we publish the edited article. We will replace this *Accepted Manuscript* with the edited and formatted *Advance Article* as soon as it is available.

You can find more information about *Accepted Manuscripts* in the [Information for Authors](#).

Please note that technical editing may introduce minor changes to the text and/or graphics, which may alter content. The journal's standard [Terms & Conditions](#) and the [Ethical guidelines](#) still apply. In no event shall the Royal Society of Chemistry be held responsible for any errors or omissions in this *Accepted Manuscript* or any consequences arising from the use of any information it contains.

1  
2  
3  
4  
5  
6  
7  
8  
9  
10  
11  
12  
13  
14  
15  
16  
17  
18  
19  
20  
21  
22  
23  
24  
25  
26  
27  
28  
29  
30  
31  
32  
33  
34  
35  
36  
37  
38  
39  
40  
41  
42  
43  
44  
45  
46  
47  
48  
49  
50  
51  
52  
53  
54  
55  
56  
57  
58  
59  
60

# Correlating enzyme density, conformation and activity on nanoparticle surface for high functional bio- nanocomposite

*Bedabrata Saha,<sup>a</sup> Jiban Saikia,<sup>b</sup> Gopal Das<sup>a,b\*</sup>*

<sup>a</sup>Centre for the Environment, Indian Institute of Technology Guwahati, Assam-781039, India

<sup>b</sup>Department of Chemistry, Indian Institute of Technology Guwahati, Assam-781039, India

Email: gdas@iitg.ac.in

**Keywords:** CuS nanoparticles; protein-nanoparticle interaction; surface crowding; trypsin activity; enzyme immobilization; enzyme kinetics.

**RECEIVED DATE (to be automatically inserted after your manuscript is accepted if required according to the journal that you are submitting your paper to)**

**Abstract**

The biological activity of immobilized enzyme is central to the performance of different nanoparticle mediated enzymatic assays, where enzymatic conversion can be used for label-free analyte detection. In this article we have addressed two significant aspect of enzyme-nanoparticle interaction. First, we have developed copper sulfide (CuS) nanoparticles, with an average diameter of 25 nm, as a potential enzyme-interface, using trypsin protease as a model enzyme. CuS nanoparticles showed high trypsin immobilization capacity up to  $14.0 \text{ mg m}^{-2}$  with significant retention of native enzymatic activity (75%-98%) in room temperature, even beyond calculated tightly packed monolayer coverage (which is around  $4.1 \text{ mg m}^{-2}$ ). Second, we report a quantitative correlation between the structure-functional relationship and the density of immobilized trypsin on nanoparticle surface. The in-situ conformation of immobilized trypsin could be analyzed well by fluorescence, circular dichroism and FT-IR spectroscopic measurements, due to the small size of the nanoparticles. Trypsin molecules appear to retain their close-native tertiary and secondary structural features (with a small loss of 1-2% of helical content) in the entire surface density range ( $2.0 - 14.0 \text{ mg m}^{-2}$ ) on CuS nanoparticles. However, interestingly, at low surface coverage ( $2.0 \text{ mg m}^{-2}$ ), immobilized trypsin retains almost 98% of its native enzymatic activity, leading to a highly functional bio-nanocomposite. While at higher surface coverage, the enzyme activity decreases to 77%, indicating the influence of steric crowding. Further, the high functionality of immobilized trypsin at low surface density on CuS nanoparticle was also supported by extracting the kinetic parameters of enzymatic activity.

## Introduction

Recent development in bio-nanotechnology have a large socioeconomic impact in bio-medical industrial sectors, as the use of nanomaterials is constantly increasing in the industrial activities such as in biosensing, diagnostics, biomedicine and therapeutics.<sup>1,2</sup> The interaction of protein/enzyme molecules with nanomaterials is the core of such applications; where the surface activity of immobilized proteins/enzymes is crucial for the assembly of interfacial protein constructs.<sup>3,4</sup> However, not much is investigated on how different factors collectively influence the activity of immobilized enzyme, especially on nanoparticle surface. Upon interaction with nanoparticles, enzyme molecules may alter its conformation, expose new epitopes on the protein surface, or even get perturbed from its normal function.<sup>5</sup> In general, different parameters can influence the conformation and the surface activity of immobilized enzymes likely, immobilization techniques and physico-chemical parameters, surface charge of nanoparticle and the enzyme molecules, surface packing density of immobilized enzymes, roughness of the nanoparticles etc. Surface density of immobilized enzyme molecules can be a significant parameter in terms of achieving desired enzyme activity on nanoparticle surface, as molecular crowding on surface can directly influence enzyme conformation and subsequently its activity. Although there are reports on different immobilization techniques to achieve high enzyme activity,<sup>3</sup> the in-depth correlation between the important parameters likely the activity, conformation and the density of the enzyme molecules, is still not well established especially on nanoparticle surface. It will be of great scientific interest to know this correlation of enzyme density, structure and function at nano-interface under relevant physico-chemical conditions, for real-time applications such as bio-sensing or proteomics.

The choice of nanomaterials as enzyme carrier is another important aspect for immobilized enzyme activity. Surface area, roughness and chemical groups of nanomaterials play an important role in interaction with enzyme molecules. In this regard, we have chosen the sulfur based nanomaterial, copper sulfide (CuS), for interaction of enzyme molecules. Copper sulfides exist as a range of stable and metastable phases ranging between copper 'poor' CuS (covellite) to copper 'rich' Cu<sub>2</sub>S (chalcocite) at

1 room temperature, common  $\text{Cu}_x\text{S}$  phases are  $\text{Cu}_{1.75}\text{S}$ (anilite),  $\text{Cu}_{1.8}\text{S}$ (digenite) and  $\text{Cu}_{1.94}\text{S}$  (djurleite).<sup>6,7</sup>  
2  
3 Although copper sulfides has been studied widely in semiconductors, solar cell materials, and as  
4  
5 catalyst,<sup>8-11</sup> it has not been studied extensively as bio-interface. Presence of sulfur on the surface can  
6  
7 make it a suitable tool to interact with biomolecules, which can bind effectively with the thiol based  
8  
9 amino acid side groups (like cysteine) of a protein. Some recent studies have also indicated the  
10  
11 possibility of using CuS as a biomolecular support, facilitating different biological applications such as  
12  
13 cancer cell cytotoxicity,<sup>12</sup> tissue imaging<sup>13</sup> etc. Moreover, the catalytic property of CuS can be utilized  
14  
15 itself as a label for detection, which will be interesting for developing 'label-free' biosensing assays. In a  
16  
17 recent study, Zhu *et al.* have demonstrated a sensitive biosensing of prostate specific antigen (up to 0.1  
18  
19 pg mL<sup>-1</sup>), using target specific antibody coated CuS nanoparticles as a label.<sup>14</sup> These results reinforce the  
20  
21 scientific interest to investigate in-depth interaction features of protein molecules with CuS  
22  
23 nanoparticles, from which we can extrapolate suitable parameters for developing functional bio-  
24  
25 nanocomposites with desired activity for above mentioned biotechnological applications. Herein, we  
26  
27 have used the trypsin protease as a model protein for the interaction with CuS nanoparticles. Trypsin is a  
28  
29 medium-sized globular protein which itself has a significant biotechnological applications such as in  
30  
31 proteomics, tissue culture, food processing and nanomedicine.<sup>15-17</sup> Trypsin cleaves peptide bonds at the  
32  
33 carboxylic groups of arginine, lysine, and ornithine, and works optimally at pH 7.5-8.5.<sup>18</sup>  
34  
35  
36  
37  
38  
39

40 In this article we have addressed two important aspect of protein-nanoparticle interaction. First, we have  
41  
42 studied how the surface density, conformation and activity of immobilized enzyme molecules  
43  
44 interrelates quantitatively on a nanoparticle surface; and second, we have demonstrated the potential  
45  
46 application of CuS nanoparticle as an enzyme carrier, with high retention of enzymatic activity  
47  
48 facilitated by simple physisorption. Physisorption of enzymes can discard the requirement of any  
49  
50 additional chemical modification/labeling of the protein molecules for immobilization, which facilitates  
51  
52 a much simpler strategy for protein immobilization. Trypsin molecules were physisorbed on CuS  
53  
54 nanoparticles at different density and different physico-chemical parameters (*viz.* available surface area  
55  
56 and temperature), and subsequently subjected to conformational and activity analysis. Due to smaller  
57  
58  
59  
60

1 hydrodynamic diameter of CuS nanoparticles, it does not significantly scatter or absorb light, therefore  
2 we could directly analyze the in-situ conformation and activity of immobilized trypsin using different  
3 spectroscopic techniques. Further we have also extracted the kinetic parameters to support the high  
4 functionality of immobilized trypsin in situ, by using the standard Michaelis-Menten kinetic model.  
5  
6  
7  
8  
9

## 10 11 **Experimental**

12 **Materials.** Cu(CH<sub>3</sub>COO)<sub>2</sub>, pyridine-2,3-dicarboxylic acid (PDA), Tris and all the other components  
13 used for buffer preparation, were purchased in analytical grade from *Merck India Ltd.*  
14  
15  
16  
17

18 **Enzyme.** Lyophilized trypsin from porcine pancreas (1:250, crystal structure is illustrated in Scheme 1a,  
19 1b) and its substrate N<sub>α</sub>-Benzoyl-L-arginine ethyl ester hydrochloride (BAEE) were purchased from  
20 *Sigma Chemicals*, USA. Prior to each experiment, fresh aqueous enzyme solutions of different  
21 concentrations were prepared in 10 mM Tris-HCl buffer (pH 8.0) containing 10 mM of CaCl<sub>2</sub>. The use  
22 of CaCl<sub>2</sub> helps to prevent the autolysis of the enzyme as well as maintain its high activity. All the  
23 solvents used in this study were of spectroscopy grade and the distilled water and deionized water  
24 (Milli-Q system at 18.2 MΩ, Millipore, USA) was used in all experiments.  
25  
26  
27  
28  
29  
30  
31  
32

33 **Synthesis and characterization of CuS nanoparticles.** CuS nanoparticles were prepared via passing  
34 H<sub>2</sub>S through a copper-acid complex solution. Briefly, aqueous solution of Cu(CH<sub>3</sub>COO)<sub>2</sub> and pyridine-  
35 2,3-dicarboxylic acid (PDA) was mixed in a molar ratio of 1:2 to form a Cu-PDA complex, which  
36 readily precipitates out from the solution. This Cu-PDA complex was used as precursor template to  
37 synthesize ultrafine CuS nanoparticles. The precipitated complex was further washed and re-dissolved  
38 into basic aqueous medium by slow and continuous addition of piperidine. H<sub>2</sub>S gas was then passed  
39 through this Cu-PDA complex solution in a controlled manner under vigorous stirring for 30 min, and  
40 stirred additionally for 30 min. A colloidal greenish-black suspension was formed by this process, which  
41 was separated by high speed centrifuge at 15000 rpm for 15 min. Precipitate was further re-suspended  
42 with Milli-Q water and methanol to wash several times for removing the impurities. Finally, the washed  
43  
44  
45  
46  
47  
48  
49  
50  
51  
52  
53  
54  
55  
56  
57  
58  
59  
60

1 CuS nanoparticles were collected after drying under vacuum and used for further interaction studies with  
2 trypsin.  
3

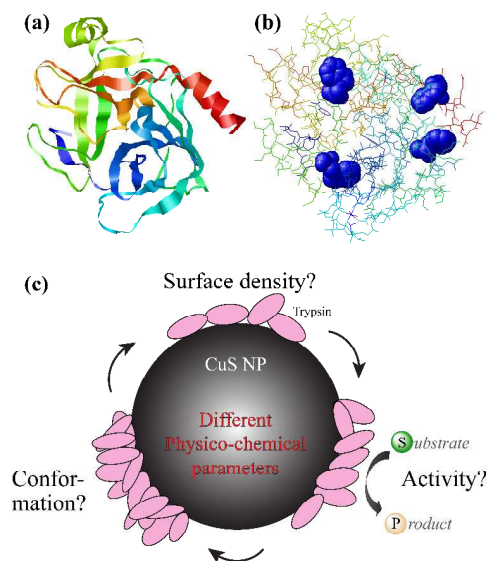
4 Synthesized nanoparticles were characterized in transmission electron micrograph (TEM), scanning  
5 electron microscope (SEM), FT-IR, powder XRD and thermogravimetric analysis (TGA). Surface area  
6 of the nanoparticles were measured by BET procedure by measuring the N<sub>2</sub> adsorption. The detailed  
7 characterization techniques are given in the supporting information.  
8  
9

10 **Adsorption of trypsin.** Batch adsorption experiments of trypsin on CuS nanoparticles were performed at  
11 pH 8.0 (with 10 mM Tris-HCl buffer), at a function of time, system temperature, and trypsin and CuS  
12 nanoparticle concentration. The amount of adsorbed enzyme was calculated by measuring the  
13 supernatant trypsin concentration using Bradford assay and measuring the absorbance at 280 nm. The  
14 detailed adsorption experiments of trypsin-CuS interaction and calculations are described in the  
15 supporting information, and summarized in Scheme 1c.  
16  
17  
18  
19  
20  
21  
22  
23  
24  
25  
26  
27

28 **Conformational analysis of trypsin interaction.** The tertiary conformation of native trypsin and  
29 immobilized at different physico-chemical parameters were measured using fluorescence emission  
30 spectroscopy. Trypsin-CuS interaction was also analyzed by measuring the fluorescence anisotropy and  
31 time-resolved fluorescence for understanding the adsorption induced molecular alteration of trypsin  
32 molecules. Further, we have analyzed the secondary conformation of immobilized trypsin as a function  
33 of available nanoparticle surface area and immobilized trypsin density, using circular dichroism and  
34 Fourier transformed infrared (FT-IR) spectroscopy. These experimental details and data analysis  
35 methodologies are described in detail in the supporting information.  
36  
37  
38  
39  
40  
41  
42  
43  
44  
45  
46

47 **Enzymatic activity of trypsin.** The enzymatic activity assay of free and immobilized trypsin (at different  
48 surface density and temperature) was analyzed by using BAEE (*N*- $\alpha$ -benzoyl-L-arginin-ethyl ester) as  
49 substrate<sup>19</sup> in 50mM Tris-HCl buffer (pH 8.0). Here we present the relative specific activity (%) retained  
50 by immobilized enzyme compared to the same amount of the native enzyme in solution, for better  
51 understanding of the loss in enzyme activity upon adsorption. Further, the enzyme kinetic study was  
52 performed by adding different amount of BAEE (0.2–1.5 mM) and by analyzing using Michaelis-  
53  
54  
55  
56  
57  
58  
59  
60

Menten kinetic model. The detailed experimental procedure of enzyme activity kinetics is described in supporting information.



**Scheme 1.** Crystal structure of trypsin molecule: (a) distribution of  $\alpha$ -helical and  $\beta$ -sheet elements as obtained from crystallographic data (<http://www.rcsb.org>). (b) Blue space-filled indicate the location of four tryptophan moieties in the three dimensional structure of trypsin molecule. (c) Brief schematic illustration of the experiments performed in this study: the trypsin molecules were immobilized on CuS nanoparticles at different physico-chemical conditions and the in-situ correlation of immobilized surface density, conformation and activity has been established.

## Result and Discussion

**Characterization of CuS nanoparticles.** Transmission electron microscopic (TEM) images (Fig. 1a) and corresponding particle size distribution analysis (Fig. 1b) revealed the near-spherical shape of synthesized CuS nanoparticles with a size distribution in the range of 20–50 nm, which is fairly polydisperse. One control experiment has been also done by passing the  $\text{H}_2\text{S}$  gas to only  $\text{Cu}(\text{CH}_3\text{COO})_2$  solution, which resulted in bulk precipitation of CuS from solution. Due to the strong coordinating ability of carboxylate groups of PDA, it can bind strongly with metal center of  $\text{Cu}^{2+}$ .<sup>20,21</sup> Therefore, the bi-dentate ligand PDA acted as a stabilizing agent in preparation of CuS nanoparticle. The elemental



analysis of CuS nanoparticles with energy dispersive X-ray (EDX) spectra reveals the presence of only Cu and S in the CuS nanoparticle samples (Supporting Information, Fig. S2).

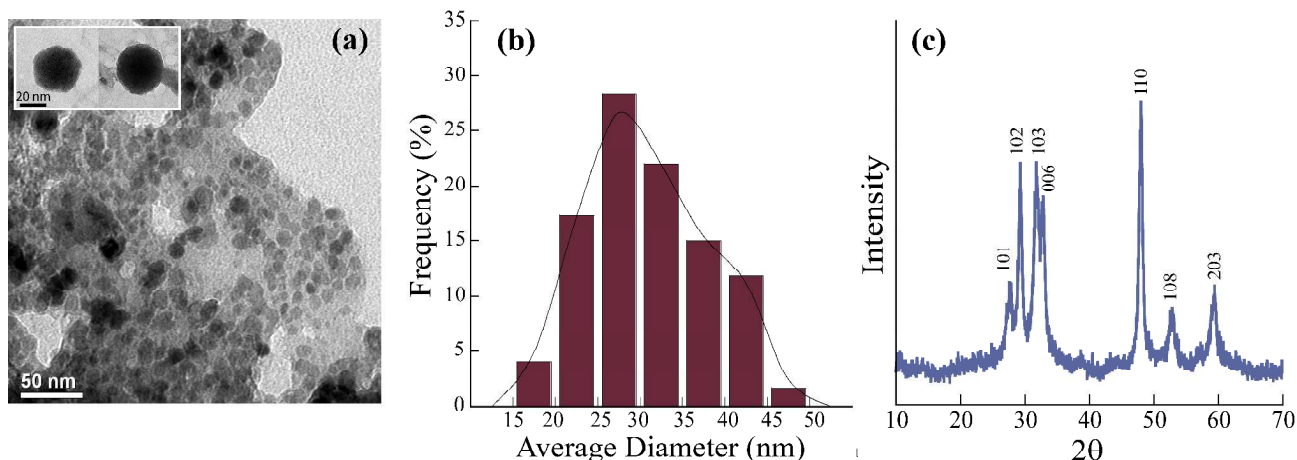


**Fig. 1.** Characterization of CuS nanoparticles: (a) TEM images (inset: individual nanoparticles) (b) size distribution analysis and (c) powder XRD (PXRD) spectra of synthesized CuS nanoparticles.

All peaks of the powder X-ray diffraction (PXRD) data shows the formation of crystalline nanoparticle (Fig. 1c), and the peaks are matching well with the covellite phase of CuS (JCPDS file no. 00-006-0464).<sup>22</sup> The crystalline nature of the CuS nanoparticles was also confirmed from the SAED analysis of the TEM images (Supporting information, Fig. S3a). The average crystallite size of CuS nanoparticles was calculated  $\sim 25$  nm, using the Debye–Scherrer equation from the fwhm of the strongest peak, is consistent with the TEM and size distribution analysis. The  $N_2$  adsorption isotherm of the BET analysis represents the type II isotherm according to Brunauer’s classification (Supporting Information, Fig. S3b). From analysis, we found that CuS nanoparticles have a high specific surface area of  $60 \text{ m}^2 \text{ g}^{-1}$  and a pore volume of  $0.449 \text{ cm}^3 \text{ g}^{-1}$ . FT-IR spectra (Supporting Information, Fig. S4a) show the characteristic peaks of CuS. The weak metal-sulfur band of CuS nanoparticles could be observed at  $\sim 617 \text{ cm}^{-1}$  region.<sup>23</sup>

Thermal decomposition of CuS nanoparticles (in  $N_2$  atmosphere), in the range of 25-100  $^\circ\text{C}$  was also studied (Supporting Information, Fig. S4b). At temperature range 100-150  $^\circ\text{C}$  the observed weight loss is mainly due to the release of water vapour associated with the material. The CuS nanoparticles undergo a desulfurization above 400  $^\circ\text{C}$  to give the product  $\text{Cu}_2\text{S}$ . Therefore, a further weight loss was

1 observed in the temperature range of 300-450 °C, which is due to this decomposition of CuS to Cu<sub>2</sub>S  
2 and release of sulfur that occurred up to 430 °C (Eq. 1).<sup>24</sup>  
3  
4



5  
6  
7  
8 This decomposition pattern is in good agreement with the previous reports.<sup>25</sup> Moreover; the DSC pattern  
9 (Supporting Information, Fig. S4b) of CuS nanoparticles in this temperature range also reflects a change  
10 in phase from CuS to Cu<sub>2</sub>S at this temperature range. The theoretical and measured (from TGA graph)  
11 weight loss of CuS nanoparticles based on Eq. 1, was found similar (16.8% and 16.6% respectively),  
12 which supports the chemical characteristics of formation of CuS nanoparticles.  
13  
14  
15  
16  
17  
18  
19  
20  
21

22 ***Time dependent interaction of trypsin with CuS nanoparticles.*** The kinetics of trypsin interaction with  
23 CuS nanoparticles (at pH 8.0, with 0.5 mg mL<sup>-1</sup> CuS and 1.0 mg mL<sup>-1</sup> trypsin) was studied for a duration  
24 of 6 h, and the time dependent adsorption capacity of trypsin is shown in Fig. 2a. Initially the adsorption  
25 capacity of trypsin scales up fast, leading to a plateau beyond 2 h, and thereafter reached steady state  
26 around the adsorption capacity of 7.0 mg m<sup>-2</sup> within 4-5 h. More than 80% of the final capacity of  
27 trypsin was adsorbed within first 1 h. On a ‘soft’ surface (according to HSAB principle<sup>26</sup>) like CuS,  
28 binding of proteins may principally govern by electrostatic interactions. Previous studies reported the  
29 surface potential analysis (ζ-potential) of different CuS materials.<sup>27</sup> Covellite phase CuS nanomaterials  
30 was found to have an isoelectric point (IEP) at around pH 3.0. On the other hand, the IEP of molecular  
31 trypsin is around pH 9.0. Therefore, at pH 8.0 the CuS surface becomes negatively charged and the  
32 trypsin molecule is partially protonated, which can lead to a strong electrostatic bonding and resulted in  
33 high adsorption capacity for trypsin. In addition with electrostatic interaction, physisorption of trypsin  
34 can also govern via formation of hydrogen bonds between the protein molecules and nanoparticle  
35 surface. Moreover, having the sulfur group on the CuS surface may also facilitate the enzyme  
36 immobilization via di-sulfide bonds using the side chains of thiol containing amino acid of trypsin  
37 molecule like cysteine.<sup>28</sup>  
38  
39  
40  
41  
42  
43  
44  
45  
46  
47  
48  
49  
50  
51  
52  
53  
54  
55  
56  
57  
58  
59  
60

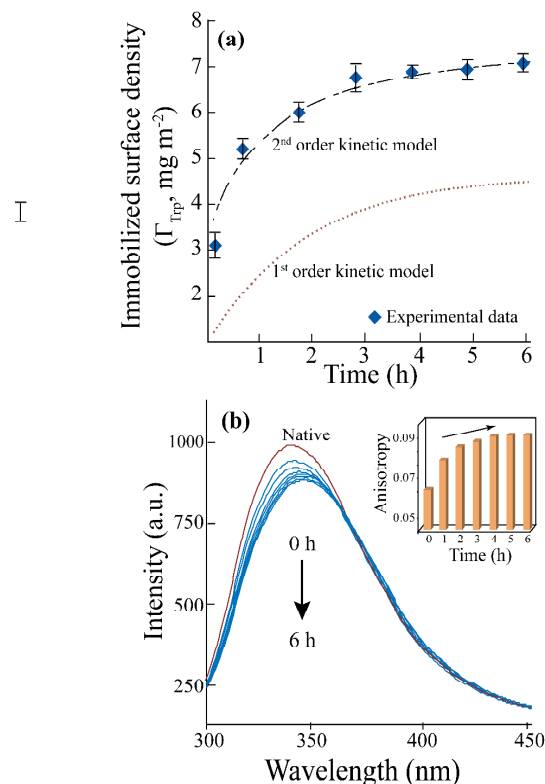


**Fig. 2.** Time dependent interaction of trypsin with CuS nanoparticles: (a) Immobilized trypsin density on CuS nanoparticles as a function of time. First order and second order kinetic equation model have been fitted (two different dotted lines) with the experimental data to extract the kinetic parameter of adsorption. (b) The steady state fluorescence emission spectrum in red represents the native trypsin's emission intensity, and the subsequent blue spectra represents the fluorescence emission intensity upon interaction with CuS nanoparticles as function of time; (inset) anisotropy values of trypsin interaction with CuS nanoparticles as a function of time.

First order and second order kinetic model was fitted with the experimental kinetics data of trypsin adsorption on CuS nanoparticles, and the kinetic parameters were calculated for both cases (Supporting Information, Fig. S5, Table S1). Second order kinetic model showed a higher correlation coefficient ( $R^2$ ) of 0.998 than that of first order model ( $R^2 = 0.940$ ), which can be attributed to the actual heterogeneous distribution of CuS surface. The experimental data were compared together with pseudo first and second

1 order models (Fig. 2a). The second order model matches well with the experimental data, while the first  
2 order model was far underestimated the actual amount of trypsin immobilized.  
3

4  
5 Further, the tertiary conformation of immobilized trypsin on CuS nanoparticles as a function of time  
6 was analyzed with steady state fluorescence spectroscopy. Trypsin molecules contain four tryptophan  
7 (Trp) moieties that can be used as intrinsic fluorophores (Scheme 1b). The  $\lambda_{\text{max}}$  of native trypsin  
8 emission spectrum in solution is characterized at 345 nm which indicates that specific tryptophan(s) of  
9 trypsin are partly exposed to the aqueous solvent (Fig. 2b). This observation is consistent with the  
10 reported native conformation of trypsin in solution.<sup>29</sup> Upon binding on CuS surface, the fluorescence  
11 intensity of trypsin quenched partially with time, with a small red shift (Fig. 2b).  
12  
13  
14  
15  
16  
17  
18  
19  
20

21 Partial decrease in fluorescence intensity is possible when the tertiary conformation of adsorbed trypsin  
22 molecules alter in such a way that the Trp moieties occupy a positions in close proximity of other  
23 fluorescence-quenching amino acids. Among different amino acids, cysteine (Cys) is strong quenchers  
24 of tryptophan fluorescence and, therefore, in the native state tryptophan moieties neighboring to the Cys  
25 residues do not significantly contribute to the overall fluorescence emission.<sup>30</sup> In trypsin's three  
26 dimensional molecular structure, different Cys residues are in close proximity of the three Trp moieties  
27 (Trp 141, Trp 215 and Trp 237) of the enzyme. Only Trp 51 locates relatively far from the cysteine  
28 group, which therefore can contribute the majority of the fluorescence intensity.<sup>30,31</sup> However, the  
29 quenching of the fluorescence intensity slows down with time and saturates once steady state reaches  
30 (spectra from 4-6 h). This indicates upon initial binding on nanoparticle surface, trypsin molecules adopt  
31 partial loss in its tertiary conformation, and did not underwent total denaturation or drastic  
32 conformational change. Therefore, extensive molecular rearrangements of the trypsin molecule are not  
33 likely to be the major driving force for strong adsorption of trypsin on CuS surface. The displacement of  
34 trypsin molecule from CuS surface (after reaching steady state), has also been studied by re-dispersing  
35 the enzyme loaded nanoparticles into the enzyme-free buffer (10 mM Tris-HCl buffer) solution. A time  
36 dependent study up to 2 h showed no detectable trypsin molecules in the solution as obtained from the  
37  
38  
39  
40  
41  
42  
43  
44  
45  
46  
47  
48  
49  
50  
51  
52  
53  
54  
55  
56  
57  
58  
59  
60

1  
2  
3  
4  
5  
6  
7  
8  
9  
10  
11  
12  
13  
14  
15  
16  
17  
18  
19  
20  
21  
22  
23  
24  
25  
26  
27  
28  
29  
30  
31  
32  
33  
34  
35  
36  
37  
38  
39  
40  
41  
42  
43  
44  
45  
46  
47  
48  
49  
50  
51  
52  
53  
54  
55  
56  
57  
58  
59  
60

Bradford assay and absorbance at 280 nm, which indicates a strong and stable interaction of trypsin molecules with CuS surface.

The fluorescence anisotropy of trypsin binding on CuS surface as a function of time has also been measured (Fig. 2b, inset). The anisotropy value of native trypsin in solution was found 0.064 which increases up to 0.085 upon binding on CuS surface. Increase in anisotropy values indicates the increased rigidity in the surrounding environment of the fluorophores upon binding on CuS surface. The increased anisotropy value can be attributed to the imposed motional restriction on the different fluorophores of trypsin, due to the adsorption. However, the anisotropy value saturates after adsorption capacity reaches steady state. This indicates no significant alteration in three dimensional structures further, which is a similar observation compared to previous steady state fluorescence analysis.

***Binding and conformational analysis of trypsin at different available nanoparticle surface area.***

Binding of trypsin on CuS surface was studied at increasing available nanoparticle surface area, by adding different concentration of CuS nanoparticles to trypsin at room temperature. An increasing concentration of CuS nanoparticles (0.2 – 1.0 mg mL<sup>-1</sup>) was added to a fixed amount of trypsin (0.5 mg mL<sup>-1</sup>), to generate a range of available surface area from 120×10<sup>-4</sup> to 600×10<sup>-4</sup> m<sup>2</sup> mL<sup>-1</sup>. The available surface area for trypsin binding was calculated approximately from the nanoparticle concentration (mg mL<sup>-1</sup>) and its specific surface area (m<sup>2</sup> g<sup>-1</sup>). The actual surface area can vary from this calculated values, due to the size distribution, and/or partial aggregation of nanoparticles locally. The immobilized surface density of trypsin ( $\Gamma_{\text{trp}}$ ) scales down from 34.2 mg m<sup>-2</sup> to 7.7 mg m<sup>-2</sup> with the increase in available nanoparticle surface area up to 600×10<sup>-4</sup> m<sup>2</sup> mL<sup>-1</sup> (Supporting Information, Fig. S6).

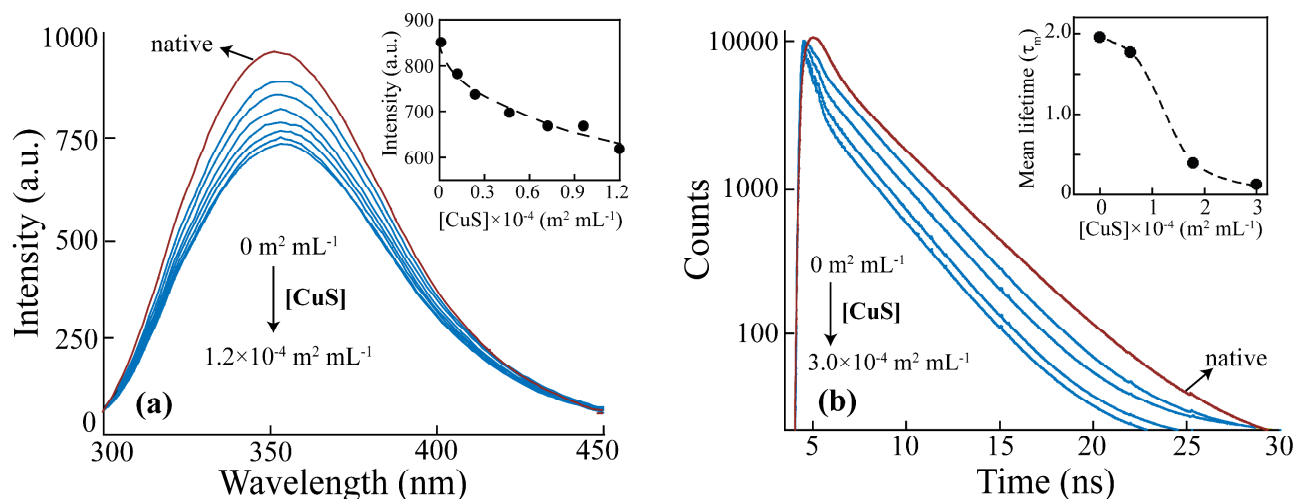


**Fig. 3.** Fluorescence analysis of trypsin-CuS binding as a function of total available nanoparticle surface area: (a) Steady state fluorescence spectroscopy showed quenching of emission intensity with the increase of CuS nanoparticle concentration. (inset) Maximum emission intensity ( $\lambda_{\max}$ ) at 345 nm as a function of available CuS nanoparticle surface area. (b) Time resolved fluorescence spectra of trypsin interaction with increasing CuS concentration. (inset) Calculated mean lifetime ( $\tau_m$ ) of trypsin molecules as a function of available CuS nanoparticle surface area.

**Steady state and time resolved fluorescence spectra.** Tertiary conformation of immobilized trypsin as a function of total available nanoparticle surface area was also studied using steady state and lifetime fluorescence spectroscopy. A lower CuS nanoparticle concentration range was used ( $0 - 5 \mu\text{g mL}^{-1}$ , corresponding up to  $3 \times 10^{-4} \text{ m}^2 \text{ mL}^{-1}$ ) for the fluorescence analysis of trypsin-CuS binding, compared to the binding capacity studies ( $120 \times 10^{-4}$  to  $600 \times 10^{-4} \text{ m}^2 \text{ mL}^{-1}$ , as described in the previous paragraph); which is mainly to minimize the optical scattering/absorbance by CuS nanoparticles at higher concentration. With the increase in available surface area ( $0$  to  $1.2 \times 10^{-4} \text{ m}^2 \text{ mL}^{-1}$ ), the steady state fluorescence intensity quenches partially (Fig. 3a), which indicates a partial unfolding of trypsin tertiary structure upon increasing concentration of CuS. A plot of  $\lambda_{\max}$  (at 345 nm) of Trp emission spectra as a function of available CuS surface area shows an almost linear decrease in fluorescence emission

1 intensity of immobilized enzymes with the increase in available nanoparticle surface area (Fig. 3a,  
2 inset).

3  
4 Time resolved fluorescence spectroscopy of trypsin molecules, upon interaction with CuS nanoparticles  
5 was analyzed by measuring the fluorescence lifetime of the Trp moieties as a function of total available  
6 nanoparticle surface area. The time-resolved decay of trypsin was taken at an emission wavelength of  
7 around 345 nm ( $\Delta\lambda = \pm 5$  nm). The sums of two exponential decay model was fitted well with the  
8 fluorescence lifetime data, with a  $\chi^2$  value close to 1.00 (utilizing Eq. S3, Supporting information). The  
9 time resolved decay profiles of native trypsin was changed progressively upon interaction with the  
10 increase in available surface area for binding (Fig. 3b). The individual lifetime values ( $\tau_1$  and  $\tau_2$ ) and the  
11 amplitudes ( $\alpha_1$  and  $\alpha_2$ ) were calculated<sup>32</sup> from the bi-exponential fit (Supporting Information, Table S2),  
12 in addition with the mean lifetime values ( $\tau_m$ ) which was calculated using Eq. S4 (supporting  
13 information). The mean lifetime ( $\tau_m$ ) of native trypsin is close to 2 ns which scales down up to 0.11 ns  
14 upon interaction with the increased available nanoparticle surface area up to  $3.0 \times 10^{-4}$  m<sup>2</sup> mL<sup>-1</sup>  
15 (Supporting Information, Table S2). At higher available surface area ( $> 0.6 \times 10^{-4}$  m<sup>2</sup> mL<sup>-1</sup>), the mean  
16 fluorescence lifetime decays rapidly (Fig. 3b, inset). The decrease in mean lifetime values ( $\tau_m$ ) of the  
17 fluorophore can be attributed to the alteration of polarity of the environment surrounding the  
18 fluorophore; which indicates partial unfolding of trypsin and exposure of fluorophore to the aqueous  
19 solvent upon binding on CuS nanoparticle surface.  
20  
21  
22  
23  
24  
25  
26  
27  
28  
29  
30  
31  
32  
33  
34  
35  
36  
37  
38  
39  
40  
41  
42  
43  
44

45 **Circular dichroism spectra.** Secondary conformation of trypsin interaction as a function of available  
46 CuS nanoparticle surface area have been investigated by far circular dichroism (CD) spectroscopy. The  
47 CD spectra of native and immobilized trypsin exhibits a broad negative band having minimum molar  
48 ellipticity in the range of 200-208 nm with a shoulder at ~220 nm (Fig. 4). This is the characteristics of  
49 the enzyme like trypsin, which contains both  $\alpha$ -helices and  $\beta$ -sheets.<sup>33</sup> Analysis of CD spectra reveals  
50 that native trypsin in solution contains ~7.2%  $\alpha$ -helices, ~41.8%  $\beta$ -sheets and the rest ~51.8% of turn  
51 and other unordered elements. Although having lower signal to noise ratio, a similar shape of the CD  
52  
53  
54  
55  
56  
57  
58  
59  
60

spectra of immobilized trypsin was observed compared to that of free enzyme. Analysis with Dichroweb software reveals a comparable secondary structural elements of the immobilized trypsin with its native form, after interaction with low concentration of CuS nanoparticles ( $\leq 1.2 \times 10^{-4} \text{ m}^2 \text{ mL}^{-1}$ , Supporting Information, Table S3).

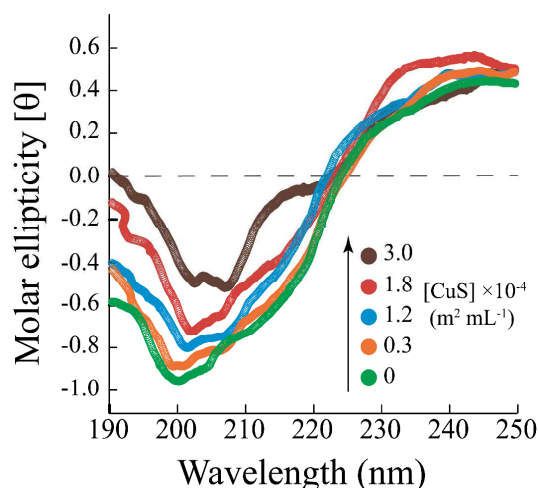


**Fig. 4.** Circular dichroism spectra of trypsin interaction with CuS nanoparticles as a function of increasing available nanoparticle surface area (by adding increased concentration of CuS nanoparticle).

At higher available nanoparticle surface area of CuS ( $\geq 2.0 \times 10^{-4} \text{ m}^2 \text{ mL}^{-1}$ ), the  $\alpha$ -helical content of immobilized trypsin was decreased partially to  $\sim 6.7\%$ . This set of data indicates that, upon interaction with CuS nanoparticles, although the tertiary conformation is partially rearranged, it marginally affects the secondary structural elements. Later in this article, we have also presented the secondary structural elements of immobilized trypsin as a function of its surface density on CuS nanoparticles.

#### ***Surface density of immobilized trypsin on CuS nanoparticles and structure-functional correlation***

***Surface density of immobilized trypsin:*** Isotherm studies at different surface density of immobilized trypsin on CuS surface was performed by adding a fix amount of CuS ( $1 \text{ mg mL}^{-1}$ , corresponding to  $60 \times 10^{-4} \text{ m}^2 \text{ mL}^{-1}$ ) to different concentration of trypsin ( $0.1 - 1.0 \text{ mg mL}^{-1}$ ) at pH 8.0 in room temperature. The steady state adsorbed amount of trypsin on CuS surface scales up with increasing initial trypsin concentration as shown in Fig. 5a. The initial high slope in the isotherm plot indicates



1 high affinity of trypsin for CuS surface, which approaches towards a plateau at higher trypsin  
2 concentration. Using the molecular dimensions of trypsin, the maximum theoretical surface  
3 concentration could be calculated. On the basis of crystallographic information (Protein Data Bank entry  
4 2PTN),<sup>29</sup> the spatial conformation of the native trypsin molecule can be approximated as an ellipsoid  
5 with dimensions of 4.8 nm × 3.7 nm × 3.2 nm (Scheme 1a, 1b). Considering that the enzyme molecules  
6 are surrounded by a hydration layer of approximately 0.2 nm, and that they adsorb in a *side-on* and *end-*  
7 *on* configuration, a tightly packed monolayer would contain around 2.4 mg m<sup>-2</sup> and 4.1 mg m<sup>-2</sup> of  
8 unperturbed trypsin molecules respectively. However, the actual surface roughness of the CuS  
9 nanoparticles will lead to a different effective surface area per nanoparticle, which can shift these  
10 numbers to somewhat higher values. However, the isotherm data reveals that in the added concentration  
11 range of trypsin, the surface density of immobilized trypsin varies from a close-monolayer coverage  
12 (~2.0 mg m<sup>-2</sup>) to a crowded tightly packed coverage (> 5 mg m<sup>-2</sup>). With higher trypsin concentration, the  
13 adsorption capacity reaches up to around 14.0 mg m<sup>-2</sup>, which is significantly higher than the calculated  
14 *end-on* monolayer coverage value for adsorbed trypsin. The isotherm graph does not show a complete  
15 plateau, which indicates the adsorption capacity can also increase further. This reveals, at higher surface  
16 density the trypsin molecules get adsorbed either by adjusting in its tertiary conformation or by forming  
17 a loosely bound multiple layer on nanoparticle surface. However, formation of multiple layer via weak  
18 molecular interaction can also lead to quick desorption of the enzyme molecules from the nanoparticle  
19 surface; however we did not observe any detectable trypsin molecules leaking out from the nanoparticle  
20 surface while re-dispersing it in enzyme free solution (also described in section 3.2). Hence, we interpret  
21 that partial conformational re-arrangement of immobilized trypsin is most likely the principal driving  
22 force at higher immobilized surface density.  
23  
24  
25  
26  
27  
28  
29  
30  
31  
32  
33  
34  
35  
36  
37  
38  
39  
40  
41  
42  
43  
44  
45  
46  
47  
48  
49  
50  
51  
52  
53  
54  
55  
56  
57  
58  
59  
60

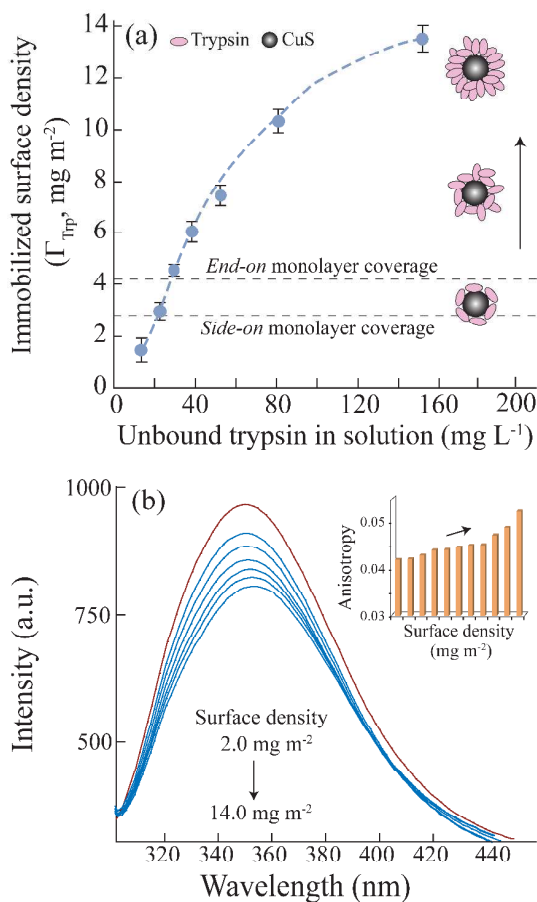


**Fig. 5.** Adsorption capacity and conformation of trypsin at different surface density: (a) Adsorption isotherm of trypsin on CuS nanoparticles at different initial trypsin concentration. Dashed line fitted through the data points represents the guide to the eye. Two horizontal lines represent the theoretical ‘side-on’ and ‘end-on’ monolayer coverage of trypsin on CuS nanoparticles. (b) Steady state fluorescence spectra and (inset) anisotropy values of immobilized trypsin as a function of surface density (2.0 – 14.0 mg m<sup>-2</sup>) on CuS nanoparticles.

**Conformational analysis at different surface density of immobilized trypsin:** We have analyzed the in-situ tertiary and secondary conformation of immobilized trypsin at different surface density on CuS nanoparticle surface by steady state fluorescence and FT-IR spectra.

**Fluorescence spectra.** The enzyme adsorbed nanoparticles were re-dispersed in the enzyme free buffer and further used in the spectroscopic studies for tertiary conformational analysis. The steady state fluorescence emission spectra of adsorbed trypsin as a function of surface density on CuS nanoparticles

1 are shown in Fig. 5b. The emission intensity of the immobilized trypsin quenched progressively with the  
2 increase in its surface density. With the increase in molecular crowding of trypsin on the CuS surface,  
3 the available surface area for binding of each trypsin molecules reduces. This could resulted in a  
4 partially perturbed tertiary conformation of immobilized trypsin so that more enzyme molecules get  
5 accommodated in close proximity on nanoparticle surface, as discussed previously. This intra-molecular  
6 and inter-molecular rearrangement of trypsin leads to spatial restriction of the fluorophore in the enzyme  
7 molecule, which resulted in partially quenched emission intensity. The anisotropy values of immobilized  
8 trypsin molecules are presented (Fig. 5b, inset) after subtracting the anisotropy values of the CuS  
9 nanoparticle solution as a background correction. Although the change in anisotropy values with  
10 increasing surface density of immobilized trypsin is slighter, it represents an increased spatial restriction  
11 of the fluorophore within the enzyme molecule. At higher trypsin surface density ( $\geq 10 \text{ mg m}^{-2}$ ), the  
12 increase in anisotropy is more rapid compared to lower surface density; this also indicates a crowding  
13 effect starts to play role more significantly on enzyme conformation in this regime. Moreover,  
14 considering the aggregation of the enzyme molecules at these concentrations, fluorescence emission  
15 spectra of free trypsin solution has also been taken for this whole concentration range. The fluorescence  
16 emission spectra of trypsin at different experimental concentration did not show any notable change,  
17 from which we assume negligible aggregation of trypsin takes place in this concentration range.

18  
19  
20  
21  
22  
23  
24  
25  
26  
27  
28  
29  
30  
31  
32  
33  
34  
35  
36  
37  
38  
39  
40  
41  
42 **FT-IR spectra.** The FT-IR spectra of lyophilized trypsin in native and adsorbed state (with different  
43 surface density on CuS nanoparticles) were taken from 4000 to 500  $\text{cm}^{-1}$ . The amide I band at  
44 1700–1600  $\text{cm}^{-1}$  region is mainly due to the C=O stretching and N–H bending vibration. The band  
45 at ~1540–1500  $\text{cm}^{-1}$  corresponds to amide II, which represents mainly the C–N stretch vibration  
46 (Supporting Information, Fig. S7).<sup>34,35</sup> Although there were no significant peaks of only CuS at amide I  
47 region of protein spectrum, the IR spectrum of trypsin immobilized onto CuS surface was analyzed after  
48 subtracting the CuS spectrum as a background correction. Further, the individual secondary structural  
49 elements of immobilized trypsin at different surface density were quantified by Gaussian deconvolution  
50  
51  
52  
53  
54  
55  
56  
57  
58  
59  
60

analysis of the amide I region (1700–1600  $\text{cm}^{-1}$ ) of the FT-IR spectra (Supporting Information, Fig. S8).<sup>36,37</sup> The Gaussian distribution peak at  $1654 \pm 2 \text{ cm}^{-1}$  was assigned to  $\alpha$ -helix, bands at  $1686 \pm 1$ ,  $1644 \pm 1$ ,  $1628 \pm 1$  and  $1625 \pm 1 \text{ cm}^{-1}$  were assigned to  $\beta$ -sheet, and all other peaks were assigned to unordered structural elements including  $\beta$ -turns, random coils, and extended chains.<sup>38</sup> Gaussian analysis reveals that native trypsin has an  $\alpha$ -helical content of  $\sim 7\%$ ,  $\beta$ -sheet of  $\sim 34\%$ , and rest  $\sim 59\%$  unordered elements (Table 1).

**Table 1.** Secondary structural content (%) of trypsin in native and different immobilized state.

	Native Trypsin	Surface coverage of adsorbed trypsin ( $\text{mg m}^{-2}$ )				
		2.0	3.8	6.0	10.3	14.0
$\alpha$ -helix (%)	$7.3 \pm 1$	$7.2 \pm 1$	$7.0 \pm 1$	$6.7 \pm 2$	$6.6 \pm 1$	$6.1 \pm 2$
$\beta$ -sheet (%)	$34.2 \pm 1$	$35.8 \pm 1$	$34.8 \pm 2$	$36.3 \pm 1$	$35.9 \pm 2$	$37.1 \pm 1$
Unorder (%)	$58.5 \pm 2$	$57.5 \pm 2$	$58.2 \pm 1$	$57.0 \pm 1$	$57.8 \pm 2$	$57.3 \pm 1$

Previous studies also reported similar secondary structural content of native trypsin.<sup>39,40</sup> The partial difference in secondary structural content of native trypsin as analyzed by FT-IR spectra and CD spectra (34%  $\beta$ -sheet and 41%  $\beta$ -sheet respectively), can be attributed to the lyophilization induced conformational change in enzyme molecule for FT-IR analysis. The FT-IR data reflects that upon adsorption on CuS surface, the trypsin molecule significantly retain its secondary structural content, throughout all the surface density range studied. Only at higher surface density ( $> 5 \text{ mg m}^{-2}$ ), a small loss of  $\alpha$ -helical structure of adsorbed trypsin was observed (around 1-2%).

**Activity of immobilized trypsin at different surface density:** The enzymatic activity of nanoparticle-bound trypsin molecules was measured at different surface density, using BAEE as substrate. The relative specific activity of nanoparticle bound trypsin was measured and presented in percents (%) compared to the same amount of native trypsin activity (Fig. 6a). At a surface density of around 2.0 mg

1 m<sup>-2</sup> almost 98% of the native enzyme activity was retained by the adsorbed trypsin molecules  
2 (Supporting information, Table S4). Noticeably, in this regime as per theoretical calculation, the  
3 immobilized trypsin molecules occupy a complete monolayer coverage on CuS nanoparticle surface.  
4  
5 Previously, we have observed a marginal loss of secondary and tertiary structure of immobilized trypsin  
6  
7 in this surface density regime (as described in section 3.4.2), which can be related to the high retention  
8  
9 of enzymatic activity. At higher surface density of adsorbed trypsin (> 5 mg m<sup>-2</sup>), partial loss in enzyme  
10  
11 activity (around 10-20%) was observed, which can be influenced by the increased alteration in the  
12  
13 tertiary conformational of enzyme molecules in this regime. This measured loss in activity of  
14  
15 immobilized trypsin can be the consequence of either the decrease in absolute number of active enzyme  
16  
17 molecules on CuS surface, or the reduced kinetic parameters of immobilized enzyme-catalysis, or both  
18  
19 together. This may indicate towards a heterogeneous distribution in the activity of immobilized enzymes  
20  
21 at higher surface density, which however, could not be quantified individually in this study. Hence, we  
22  
23 represent the activity loss of immobilized enzyme by measuring the overall product conversion by the  
24  
25 total amount of immobilized trypsin after a defined time duration. Within our experimental range, we  
26  
27 found at room temperature the activity of immobilized trypsin reduced to ~77% till the surface density  
28  
29 reaches to ~14.0 mg m<sup>-2</sup> on CuS nanoparticles (which is significantly higher than theoretical monolayer  
30  
31 coverage value). We attribute this loss of activity to the increased crowding of the enzyme molecules at  
32  
33 surface. Further, this data fitted well with a linear equation (Fig. 6a) with a correlation coefficient (R<sup>2</sup>)  
34  
35 of 0.986, signifying the linear decrease in enzyme activity on CuS nanoparticle decreases with increase  
36  
37 in its surface packing density in the studied regime. Fig. 6b represents the direct correlation between the  
38  
39 surface density, conformation and in situ enzymatic activity of immobilized trypsin. It is apparent from  
40  
41 this graph that, increasing the surface density of immobilized enzyme beyond the monolayer coverage  
42  
43 has a simultaneous influence on its in situ activity as well as in its conformation. We have also  
44  
45 performed a control experiment by incubating BAEE with bare CuS nanoparticles (without trypsin  
46  
47 immobilized), however no detectable amount of hydrolyzed product was observed upon measuring at  
48  
49 253 nm.  
50  
51  
52  
53  
54  
55  
56  
57  
58  
59  
60

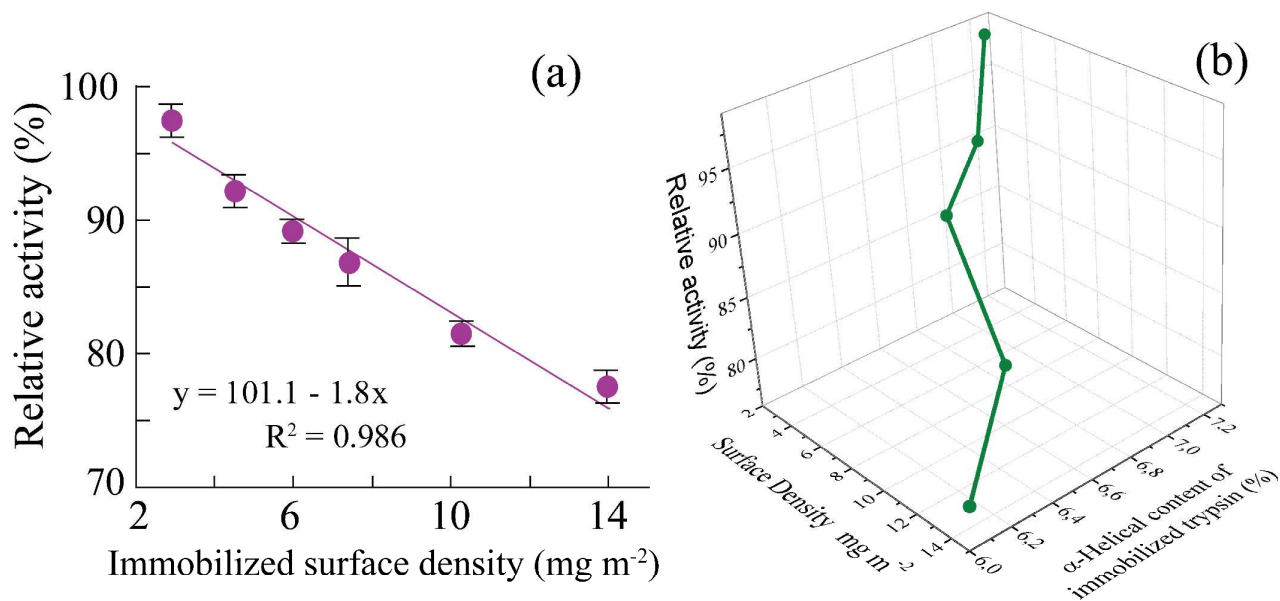


**Fig. 6.** (a) Retention of enzymatic activity of trypsin molecules as a function of immobilized surface density on CuS nanoparticles. The solid line represents a fit with a linear equation. (b) Direct correlation of surface density ( $\text{mg m}^{-2}$ ), secondary conformation ( $\alpha$ -helical content, %) and in situ activity (retention of activity, %) of immobilized trypsin on CuS nanoparticles.

In addition, we have also studied the adsorption capacity, conformation and activity of immobilized trypsin in a temperature range of 10 to 50 °C, to analyze the stability and functionality of the bio-nanocomposite. Briefly, the adsorption capacity scales down with the increase in temperature from 10 to 40 °C (from 30.2 to 14.0  $\text{mg m}^{-2}$ ), while we observed higher enzymatic activity at 40 °C (~90%). We interpret both the surface density of immobilized enzyme (which also varies at different temperature), and the temperature might have a combine influence on the activity of immobilized trypsin in the temperature range studied here. The conformational analysis using fluorescence spectroscopy and anisotropy reveals partial conformational loss of immobilized trypsin at room temperature (as discussed before), which undergoes further conformational alteration with the increase in temperature. More detailed discussion on temperature influenced interaction of trypsin with CuS nanoparticles is given in the supporting information.

### Enzyme kinetics of immobilized trypsin

The enzyme activity kinetics of immobilized trypsin was studied at a surface coverage of 2.0 mg m<sup>-2</sup> on CuS nanoparticle, and was compared with that of native enzyme molecules. The rate of enzymatic activity,  $v$  (mg mL<sup>-1</sup> min<sup>-1</sup>) was calculated following the Michaelis-Menten kinetics<sup>41</sup> given by Eq. 2:

$$v = \frac{v_{\max} \cdot [S]}{K_m + [S]} = \frac{k_{cat} \cdot [E]_T \cdot [S]}{K_m + [S]} \quad (2)$$

Where,  $[S]$  is substrate (BAEE) concentration (mM),  $v_{\max}$  is the maximum rate attained at infinite concentration of substrate, and  $K_m$  is the Michaelis-Menten constant. The term  $v_{\max}$  can be further expressed by  $k_{cat}$  and  $[E]_T$ , which is turn over number and total enzyme concentration used for kinetics study, respectively.<sup>41</sup> Fig. 7a shows the Michaelis-Menten plot for the hydrolysis of BAEE by native and immobilized enzyme at pH 8.0 and 25° C. Maximum kinetic rate ( $v_{\max}$ ) and Michaelis-Menten constant ( $K_m$ ) values for both free and immobilized enzyme were calculated (Fig. 7b, inset) from the double reciprocal linearized Lineweaver-Burk plot (by re-arranging Eq. 2).

The maximum enzyme kinetic rate ( $v_{\max}$ ) of native and immobilized trypsin was almost similar (0.042 and 0.040 mM min<sup>-1</sup> respectively). This reveals, the adsorption of trypsin on CuS surface at a low surface density (2.0 mg m<sup>-2</sup>) has a little influence on the release of the hydrolyzed product of BAEE in the rate limiting step. The Michaelis-Menten constant ( $K_m$ ) value for native trypsin was marginally decreased upon adsorption on CuS surface (0.35 mM to 0.32 mM), at low surface density (2.0 mg m<sup>-2</sup>). Although, this change is not highly significant, yet this points towards the increased affinity of the immobilized enzyme for the substrate BAEE. Upon immobilization on nanoparticle surface, the enzyme molecules can interact with the substrate molecules in the solution more rapidly, compared to the diffusion based interaction of native trypsin and substrate molecules in the solution.

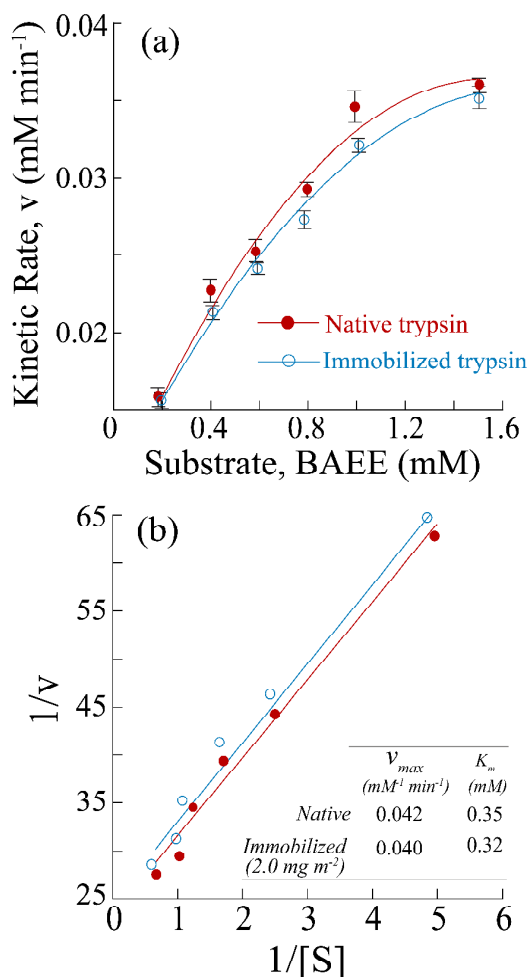


**Fig. 7.** Enzyme kinetics of native and immobilized trypsin (with 2.0 mg m<sup>-2</sup> surface density): (a) Michaelis-Menten plot with different BAEE concentration. (b) Double reciprocal Lineweaver-Burk plot of free and immobilized trypsin on CuS nanoparticles. (inset) Enzyme kinetic parameters of free and immobilized trypsin calculated from the Lineweaver-Burk plot.

## Conclusion

We have demonstrated the potential use of CuS nanoparticles in developing a high functional bio-nanocomposites using trypsin protease as a model system, with in-depth understanding of structure-functional relationship of the immobilized enzyme. We find an overall stability of the trypsin-CuS nanocomposite in terms of its conformation and activity, at different physico-chemical conditions which can closely resembles various enzymatic assay conditions. Circular dichroism, fluorescence and FT-IR spectroscopy revealed fractional loss of the conformation of trypsin molecules upon binding on CuS



1 surface. However, immobilized trypsin molecules showed a significant retention of enzymatic activity  
2 (>75% to 98%) in the different physico-chemical conditions (immobilized enzyme density, available  
3 nanoparticle surface area) at room temperature. We find that density of immobilized trypsin molecules  
4 on nanoparticle surface is a dominant parameter which considerably influences its activity, and we have  
5 established a linear relationship between the trypsin surface density and its activity. With a monolayer  
6 trypsin coverage ( $\sim 2.0 \text{ mg m}^{-2}$ ) on CuS surface, the trypsin molecules retains around 98% of its native  
7 activity. With further increase in the surface density up to  $\sim 14.0 \text{ mg m}^{-2}$ , the overall enzymatic activity  
8 of immobilized trypsin reduced to around 77%. We attribute this reduction in activity to the steric  
9 crowding of trypsin molecules on nanoparticle surface at higher immobilization density ( $> 5 \text{ mg m}^{-2}$ ),  
10 which overestimated the calculated monolayer coverage. The crowding of enzyme molecules alters the  
11 tertiary conformation of immobilized trypsin which impair its overall catalytic activity. The enzyme  
12 kinetic analysis of immobilized trypsin with low surface density ( $\sim 2.0 \text{ mg m}^{-2}$ ) at room temperature also  
13 showed similar kinetic parameters compared to the native enzyme molecules.  
14  
15  
16  
17  
18  
19  
20  
21  
22  
23  
24  
25  
26  
27  
28  
29

30 The studied trypsin interaction with CuS nanoparticles reveals two significant aspect. First, the  
31 implementation of CuS as a potential nano-interface for enzymes in different enzymatic assays, where  
32 both the enzyme molecules and CuS nanoparticles can be used as a label free marker to determine the  
33 analyte concentration. A simple physisorption of enzyme molecules with the control over the surface  
34 density of immobilize enzyme can lead to highly functional bio-nanocomposites. Moreover, high  
35 activity of immobilized trypsin can be itself promising for proteomics application. Second, in-depth  
36 understanding of the structure-functional relation of trypsin interaction with CuS nanoparticles will  
37 facilitate the extrapolation of the crucial parameters which can regulate the enzyme activity on  
38 nanoparticle surface. The next step in developing highly functional bio-nanocomposites, would be to  
39 investigate different immobilization strategy on CuS nanoparticles and its subsequent activity at defined  
40 surface density. Further it would be also scientifically significant to quantify the possible heterogeneity  
41 in activity of the immobilized enzyme molecules. This will give a complete image of how different  
42 immobilization strategies and physico-chemical conditions lead to different active fraction of  
43  
44  
45  
46  
47  
48  
49  
50  
51  
52  
53  
54  
55  
56  
57  
58  
59  
60

1 immobilized enzyme, with defined heterogeneity in activity. This knowledge can further be very useful  
2  
3 in developing various modern biotechnological applications such as enzymatic assays, diagnostics, drug  
4  
5 delivery and therapeutics.  
6  
7  
8

9  
10 **Acknowledgement.** This work was supported by CSIR and DST through grant 01-2235/08/EMR-II and  
11  
12 SR/S1/IC-01/2008, New Delhi, India. BS acknowledges Centre for the Environment and Central  
13  
14 Instrumental Facility, IIT Guwahati for providing laboratory facilities.  
15

16  
17 **Electronic Supplementary Information (ESI) Available:** Further characterization of CuS  
18  
19 nanoparticles (TEM, TGA, EDAX, BET analysis) and interaction with trypsin in terms of kinetics and  
20  
21 isotherm; conformational details by FT-IR and CD spectroscopy; influence of temperature on enzyme  
22  
23 interaction.  
24  
25  
26  
27  
28  
29

### 30 **Notes and references**

- 31  
32  
33 [1] L. Zhang, F. X. Gu, J. M. Chan, A. Z. Wang, R. S. Langer and O. C. Farokhzad, Nanoparticles in  
34  
35 medicine: therapeutic applications and developments, *Clin. Pharmacol. Ther.*, 2008, **83**, 761–769.  
36  
37  
38 [2] X. Michalet, F. F. Pinaud, L. A. Bentolila, J. M. Tsay, S. Doose, J. J. Li, G. Sundaresan, A. M. Wu,  
39  
40 S. S. Gambhir and S. Weiss, Quantum dots for live cells, in vivo imaging, and diagnostics,  
41  
42 *Science*, 2005, **307**, 538-544.  
43  
44  
45 [3] M. Mahmoudi,; I. Lynch, M. R. Ejtehadi, M. P. Monopoli, F. B. Bombelli and S. Laurent,  
46  
47 Protein–nanoparticle interactions: opportunities and challenges, *Chem. Rev.*, 2011, **111**, 5610–5637.  
48  
49  
50 [4] D. F. Moyano and V. M. Rotello, Nano meets biology: structure and function at the nanoparticle  
51  
52 interface, *Langmuir*, 2011, **27**, 10376–10385.  
53  
54  
55  
56  
57  
58  
59  
60

- 1  
2  
3  
4  
5  
6  
7  
8  
9  
10  
11  
12  
13  
14  
15  
16  
17  
18  
19  
20  
21  
22  
23  
24  
25  
26  
27  
28  
29  
30  
31  
32  
33  
34  
35  
36  
37  
38  
39  
40  
41  
42  
43  
44  
45  
46  
47  
48  
49  
50  
51  
52  
53  
54  
55  
56  
57  
58  
59  
60
- [5] I. Lynch, K. A. Dawson and S. Linse, Detecting cryptic epitopes created by nanoparticles, *Sci. STKE*, 2006, **327**, 14.
- [6] L. Isac, A. Duta, A. Kriza, S. Manolache and M. Nanu, Copper sulfides obtained by spray pyrolysis — Possible absorbers in solid-state solar cells, *Thin Solid Films*, 2007, **515**, 5755-5758.
- [7] I. Grozdanov, C. K. Barlingay and S. K. Dey, Deposition of transparent and electroconductive chalcogenide films at near-room temperatures, *Integr. Ferroelectr.*, 1995, **6**, 205-211.
- [8] W.-T. Yao and S.-H. Yu, Synthesis of semiconducting functional materials in solution: from ii-vi semiconductor to inorganic–organic hybrid semiconductor nanomaterials, *Adv. Func. Mat.*, 2008, **18**, 3357-3366.
- [9] J. S. Chung and H. J. Sohn, Electrochemical behaviors of CuS as a cathode material for lithium secondary batteries, *J. Power Sources*, 2002, **108**, 226-231.
- [10] S. Y. Kuchmii, A. V. Korzhak, A. E. Raevskaya and A. I. Kryukov, Catalysis of the sodium sulfide reduction of methylviologene by CuS nanoparticles, *Theor. Exp. Chem.*, 2001, **37**, 36-41.
- [11] M. H. Kunita, E. M. Giroto, E. Radovanovic, M. C. O. P. Goncalves, E. C. Muniz and A. F. Rubira, Deposition of copper sulfide on modified low-density polyethylene surface: morphology and electrical characterization, *Appl. Surf. Sci.*, 2002, **202**, 223-231.
- [12] H. Wang, X. Yu, C. Wang and Y. Cao, Cooperative cytotoxic activity of Zn and Cu in bovine serum albumin-conjugated ZnS/CuS nano-composites in PC12 cancer cells, *J Nanopart. Res.*, 2013, **15**, 2020-2030.
- [13] G. Ku, M. Zhou, S. Song, Q. Huang, J. Hazle and C. Li, Copper sulfide nanoparticles as a new class of photoacoustic contrast agent for deep tissue imaging at 1064 nm, *ACS Nano*, 2012, **6**, 7489-7496.

- 1 [14] Y. Zhu, J. Peng, L. Jiang and J. Zhua, Fluorescent immunosensor based on CuS nanoparticles for  
2 sensitive detection of cancer biomarker, *Analyst*, 2014, **139**, 649-655.  
3  
4  
5  
6 [15] P. S. J. Cheetham, The application of enzymes in industry. *Handbook of Enzyme Biotechnology*,  
7  
8 3rd ed.; A. Wisemann, Ed.; Ellis Horwood Ltd.: London, 1995; pp. 419-552.  
9  
10  
11 [16] J. Krenkova, N. A. Lacher and F. Svec, Highly efficient enzyme reactors containing trypsin and  
12 endoproteinase lysc immobilized on porous polymer monolith coupled to ms suitable for analysis of  
13 antibodies 2009, **81**, 2004-2012.  
14  
15  
16 [17] Q. Min, X. Zhang, R. Wu, H. Zou and J. Zhu, A novel magnetic mesoporous silica packed S-  
17 shaped microfluidic reactor for online proteolysis of low-MW proteome, *Chem. Commun.*, 2011, **47**,  
18 10725-10727.  
19  
20  
21 [18] A. J. Barrett and J. K. McDonald, *Mammalian Proteases: A Glossary and Bibliography, Vol. I,*  
22 *Endopeptidases*; Academic Press: London, 1980.  
23  
24  
25 [19] G. W. Schwert and Y. A. Takenaka, Spectrophotometric determination of trypsin and  
26 chymotrypsin, *Biochim. Biophys. Acta*, 1995, **16**, 570-575.  
27  
28  
29 [20] W. Zhang, S. Bruda, C. P. Landee, J. Parent and M. M. Turnbull, Structures and magnetic  
30 properties of transition metal complexes of 1,3,5-benzenetricarboxylic acid, *Inorg. Chim. Acta*, 2003,  
31 **342**, 193-201.  
32  
33  
34 [21] K. E. Holmes, P. K. Kelly and M. Elsegood, Honeycombs, herringbones and brick-walls; three-fold  
35 guest-dependent variation in copper trimesate complexes bearing sulfimide ligands, *Dalton Trans.*,  
36 2004, **21**, 3488-3494.  
37  
38  
39 [22] M. Nagarathinam, K. Saravanan, W. L. Leong, P. Balaya, J. J. Vittal, Hollow nanospheres and  
40 flowers of CuS from self-assembled Cu(II) coordination polymer and hydrogen-bonded complexes of N-  
41 (2-Hydroxybenzyl)-l-serine, *Cryst. Growth Des.*, 2009, **9**, 4461-4470.  
42  
43  
44  
45  
46  
47  
48  
49  
50  
51  
52  
53  
54  
55  
56  
57  
58  
59  
60

- 1  
2  
3  
4  
5  
6  
7  
8  
9  
10  
11  
12  
13  
14  
15  
16  
17  
18  
19  
20  
21  
22  
23  
24  
25  
26  
27  
28  
29  
30  
31  
32  
33  
34  
35  
36  
37  
38  
39  
40  
41  
42  
43  
44  
45  
46  
47  
48  
49  
50  
51  
52  
53  
54  
55  
56  
57  
58  
59  
60
- [23] G. Chen, B. Deng, G. Cai, W. Dong, W. Zhang and A. Xu, Synthesis, characterization, and formation mechanism of copper sulfide-core/carbon-sheath cables by a simple hydrothermal route, *Cryst. Growth Des.*, 2008, **8**, 2137-2143.
- [24] Y. Chen, L. Chen and L. Wu, Water-induced thermolytic formation of homogeneous core-shell CuS microspheres and their shape retention on desulfurization, *Cryst. Growth Des.*, 2008, **8**, 2736-2740.
- [25] E. Godocikova, P. Balaz, J. M. Criado, C. Real and E. Gock, Thermal behaviour of mechanochemically synthesized nanocrystalline CuS, *Thermochim. Acta*, 2006, **440**, 19-22.
- [26] R. G. Pearson, Hard and soft acids and bases, *J. Am. Chem. Soc.*, 1963, **85**, 3533-3539.
- [27] J. C. Liu and C. P. Huang, Electrokinetic characteristics of some metal sulfide-water interfaces *Langmuir*, 1992, **8**, 1851-1856.
- [28] A. J. van der Vlies, C. P. O'Neil, U. Hasegawa, N. Hammond and J. A. Hubbell, Synthesis of pyridyl disulfide-functionalized nanoparticles for conjugating thiol-containing small molecules, peptides and proteins, *Bioconjugate Chem.*, 2010, **21**, 653-662.
- [29] J. Walter, W. Steigemann, T. P. Singh, H. Bartunik, W. Bode and R. Huber, On the disordered activation domain in trypsinogen: chemical labelling and low-temperature crystallography, *Acta Crystallogr. B*, 1982, **38**, 1462-1472.
- [30] R. W. Cowgill, Fluorescence and protein structure: XI. Fluorescence quenching by disulfide and sulfhydryl groups, *BBA Protein Struct.*, 1967, **140**, 37-44.
- [31] S. Koutsopoulos, K. Patzsch, W. T. E. Bosker and W. Norde, Adsorption of trypsin on hydrophilic and hydrophobic surfaces, *Langmuir*, 2007, **23**, 2000-2006.
- [32] A. B. Patel, S. Srivastava and R. S. Phadke, Interaction of 7-hydroxy-8-(phenylazo)1,3-naphthalenedisulfonate with bovine plasma albumin. Spectroscopic studies, *J. Biol. Chem.*, 1999, **274**, 21755-21762.

1 [33] T. R. Transue, J. M. Krahn, S. A. Gabel, E. F. DeRose and R. E. London, X-ray and NMR  
2 characterization of covalent complexes of trypsin, borate, and alcohols, *Biochemistry*, 2004, **43**, 2829–  
3 2839.  
4  
5

6 [34] P. Schwinte, V. Ball, B. Szalontai, Y. Haikel, J. C. Voegel and P. Schaaf, Secondary structure of  
7 proteins adsorbed onto or embedded in polyelectrolyte multilayers, *Biomacromolecules*, 2002, **3**, 1135–  
8 1143.  
9  
10

11 [35] M. V. D. Weert, P. I. Haris, W. E. Hennink and D. J. A. Crommelin, Fourier Transform Infrared  
12 Spectrometric analysis of protein conformation: effect of sampling method and stress factors, *Anal.*  
13 *Biochem.*, 2001, **297**, 160-169.  
14  
15

16 [36] P. I. Haris and F. Severcan, FTIR spectroscopic characterization of protein structure in aqueous  
17 and non-aqueous media, *J. Mol. Cat. B.*, 1999, **7**, 207-221.  
18  
19

20 [37] K. Murayama and M. Tomida, Heat-induced secondary structure and conformation change of  
21 bovine serum albumin investigated by Fourier Transform Infrared Spectroscopy, *Biochemistry*, 2004,  
22 **43**, 11526-11532.  
23  
24

25 [38] K. Griebenow and A. M. Klibnov, On protein denaturation in aqueous–organic mixtures but not in  
26 pure organic solvents, *J. Am. Chem. Soc.*, 1996, **118**, 11695-11700.  
27  
28

29 [39] K. Karen Chiu, L. L. Agoubi, I. Lee, M. T. Limpar, J. W. Lowe and S. L. Goh, Effects of Polymer  
30 Molecular weight on the size, activity, and stability of PEG-functionalized trypsin, *Biomacromolecules*  
31 2010, **11**, 3688-3692.  
32  
33

34 [40] C. Velasco-Reynold, M. Navarro-Alarcon, H. L. de la Serrana, V. Perez-Valero and M. C. Lopez-  
35 Martinez, Analysis of total and dialyzable copper levels in duplicate meals by ETAAS: daily intake *Eur.*  
36 *Food Res. Technol.* 2008, **227**, 361-373.  
37  
38  
39  
40  
41  
42  
43  
44  
45  
46  
47  
48  
49  
50  
51  
52  
53  
54  
55  
56  
57  
58  
59  
60

1 [41] R. A. Copeland, *Enzymes-A practical introduction to structure, mechanism and data analysis*, 2nd  
2 ed.; Wiley-VCH: New York, 2000.  
3  
4  
5  
6  
7  
8  
9  
10  
11  
12  
13  
14  
15  
16  
17  
18  
19  
20  
21  
22  
23  
24  
25  
26  
27  
28  
29  
30  
31  
32  
33  
34  
35  
36  
37  
38  
39  
40  
41  
42  
43  
44  
45  
46  
47  
48  
49  
50  
51 -----  
52  
53  
54  
55  
56  
57  
58  
59  
60